International Journal of Biological Macromolecules 277 (2024) 134220

Contents lists available at ScienceDirect

International Journal of Biological Macromolecules

journal homepage: www.elsevier.com/locate/ijbiomac

Production and physico-chemical characterization of nano-sized collagen from equine tendon☆

Zahra Rajabimashhadi [a], Nunzia Gallo [a,b], Francesca Russo [a], Sajjad Ghiyami [a], Claudio Mele [a], Maria Elena Giordano [c], Maria Giulia Lionetto [c], Luca Salvatore [b], Francesca Lionetto [a,*]

[a] Department of Engineering for Innovation, University of Salento, via per Monteroni, Lecce, Italy
[b] Typeone Biomaterials S.r.l., Via Europa 167, 73021 Calimera, Lecce, Italy
[c] Department of Biological and Environmental Sciences and Technologies, University of Salento, via per Monteroni, Lecce, Italy

ARTICLE INFO

Keywords:
Equine collagen
Nano collagen
Ball-milling
Particle size reduction

ABSTRACT

In recent years, significant academic and commercial interest has focused on collagen derived from horse tendons, with potential applications across diverse sectors such as medicine, pharmaceuticals, and cosmetics. Nano collagen, with its enhanced wound penetration, improved cell contact, and heightened cellular regeneration and repair capabilities due to its high surface area, holds promise for a wide range of applications. In this study, we present a novel method for producing nano collagen from the equine tendon. Our approach is characterized by its speed, affordability, simplicity and environmentally friendly nature, with precise temperature-control to prevent collagen denaturation. We conducted a comprehensive characterization of the obtained samples, including assessments of morphology, chemical and thermal properties, particle size distribution and biocompatibility. Importantly, our results indicate improvements in thermal stability, and surface roughness of nano collagen, while preserving its molecular weight. These advancements expand the potential applications of nano collagen in various fields.

1. Introduction

The growing preference for biomaterials in cosmeceutical, pharmaceutical, and medical fields has spurred increased research and technological advancements in biomaterial science [1,2]. In nature, a diverse array of polymers exists, including chitosan, keratin, cellulose, hyaluronic acid, elastin, silk and collagen, many of which find employment as biomaterial for the development of products for biomedical applications [3]. Collagen, a commonly occurring protein in the extracellular matrix of vertebrates, serves a vital function in maintaining the intricate three-dimensional microarchitecture of connective tissues [4]. Among the 28 different types of collagen, the type I collagen is the most abundant. It consists of three left-handed polyproline-II chains, (referred to as 'α' chains), into a right-handed triple helix. These triple helices then further organize into fibrils and fibers [5]. Each chain is characterized by a repeating sequence of three amino acids, denoted as (Gly-X-Y)n (X is proline and Y is hydroxyproline in most cases). The intertwining of polypeptide chains occurs through the formation of hydrogen bonds and electrostatic interactions. These interactions contribute to providing the triple helix structure with stability, flexibility, and mechanical strength [6].

Nanotechnology is the industrial use of materials at atomic, molecular, and supramolecular sizes, enabling the creation of nanomaterials for various physical, chemical, and biological systems, applicable at both the nano- and macro-scales [7] altering materials in at least one dimension within this size range. Nanofibers are cylindrical structures with diameter below 1000 nm and a length-to-width ratio exceeding 50 nm [8,9]. Nano collagen, in essence, refers to collagen that has been reduced to the nano-scale. This field of collagen nanotechnology holds great promise, with ongoing advancements poised to sustain its growth in the future [10]. Nano-scaled technologies offer enhanced wound penetration and improved cell contact due to its high surface-area-to-volume ratio. Furthermore, nano collagen can aid drug distribution and establish durable environments at injury sites, thereby fostering

☆ Please cite this article as: Zahra Rajabimashhadi et al., Effect of ball milling on the structural and stability properties of nano-sized collagen from equine tendon, International Journal of Biological Macromolecules (2024), https://doi.org/10.1016/j.cviu.2024.00.000.

* Corresponding author.
E-mail address: francesca.lionetto@unisalento.it (F. Lionetto).

https://doi.org/10.1016/j.ijbiomac.2024.134220
Received 27 March 2024; Received in revised form 24 July 2024; Accepted 25 July 2024
Available online 26 July 2024

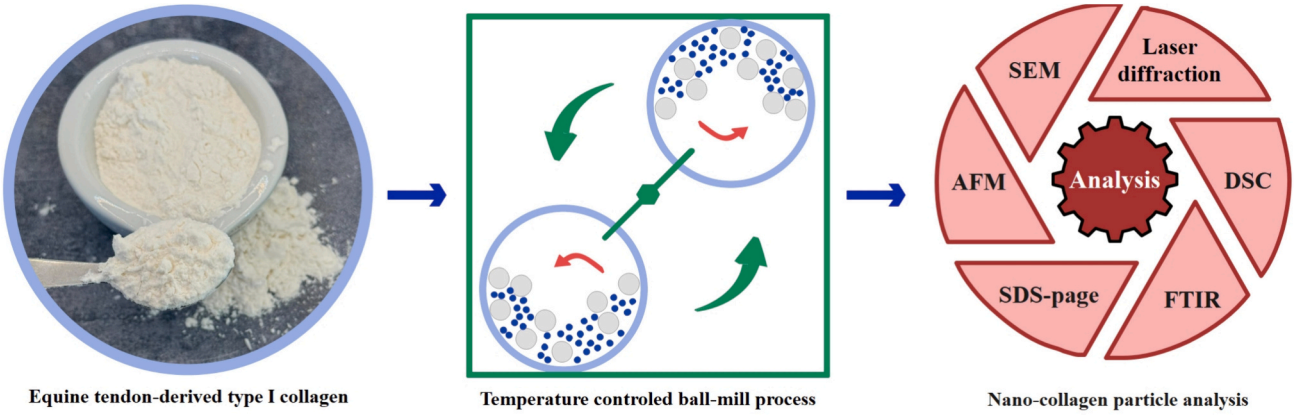

Fig. 1. Schematic representation of the milling process.

cellular regeneration and repair [11].

However, collagen-based nanotechnologies have noticeable limitations, including the limited number of commercially approved products and the lack of evidence regarding their physio-pathological consequences. Despite these drawbacks, nanotechnology-based approaches are even more of a developing trend with vast untapped potential [10]. However, further investigations are necessary to address unresolved challenges and develop safe and effective nano-based systems [12].

It is known that collagen-based dressings are effective in the healing of wounds [13,14]. In particular, powdered collagens offer distinct advantages in wound healing, as the reduced particle size efficiently adheres to and covers fissures of wounds, creating an ideal environment for the triggering of wound healing at early stages. The creation of a favorable environment for fibronectin binding, promotes the migration and growth of fibroblasts that, in turn, promotes the cascade of processes involved in the healing process [15]. The efficacy of nano collagen has been demonstrated by several studies. In 2018, a study demonstrated the efficacy of nano collagen spray derived from goldfish scales in accelerating wound healing post-incisions [16]. Additionally, also collagen nanofibers hold promise in wound healing. In 2020, collagen fibers (1 μm to 20 nm), produced by high-pressure homogenization, exhibited enhanced water barrier capacity [17].

In bone regeneration, collagen fibers ranging from 50 to 500 nm in diameter, are essential for the initial phases of bone tissue formation, by serving as a scaffold for the deposition of apatite crystals, thereby contributing to ongoing bone growth. Collagen scaffolds not only support cell differentiation and proliferation, but they also mimic the natural bone structure which is essential for the effectiveness of scaffolds in achieving optimal bone grafting outcomes [18]. In cases of dental restoration delays or poor dental health leading to unfavorable conditions in the alveolar ridge, the use of nano collagen bone powders has shown promise. Implantation of such bone grafts in patients, revealed enhanced alveolar bone mineral density and fusion between the artificial nano collagen bone and the remaining ridge. This suggests that successful alveolar ridge preservation can be achieved with the use of artificial bone made of nano collagen [19]. Furthermore, a study conducted on rabbits demonstrated that ulna bone defects can be effectively repaired by using bone combining nano collagen and allogeneic stem cells [20].

Collagen, widely utilized in cosmetics, offers significant advantages in improving skin health. Consistent use of collagen-infused beauty products has been shown to reduce signs of aging [21]. However, the use of collagen derived from mammals such as bovines and porcines in beauty products raise concerns, including objections on religious grounds and potential health risks such as the transmission of diseases like bovine spongiform encephalopathy [22]. A recent research using grouper swim bladder derived nano collagen revealed that the smaller size of nano collagen enhances its effectiveness, particularly in improving skin health, due to its superior skin barrier penetration abilities [23].

Various methods, including milling, electrospray, spray-dry, nano-emulsion, and electrospinning, can be employed to produce nano-sized collagen. Electrospray deposition, a gentle process conducted at room temperature, is particularly suitable for temperature-sensitive polymers like collagen, enabling the creation of solid nanoparticles [24]. Nano-emulsion, which involves the mixing of immiscible liquids, finds applications in cosmeceutical and pharmaceutical applications, offering benefits such as enhanced stability and absorption rates [25]. Electrospinning, an adaptable and low-cost approach, is utilized to generate nanofibers for tissue engineering applications, thanks to their closely resembling the extracellular matrix architecture [26]. Moreover, milling, a cheap approach, involves the application of mechanical energy to break down polymeric material into fine nanoparticles. It is essential to employ cooling during milling to prevent material denaturation, a phenomenon that can occur, especially with temperature-sensitive substances like collagen.

The grinding method for nano collagen production presents numerous advantages. It is cost-effective, simple, and accessible, requiring no specialized equipment. Moreover, scaling up fabrication is straightforward, making it suitable for industrial use. Grinding parameters (i. e., time and speed) allow precise control over particle size, ensuring customization for severe applications. Its efficiency allows it to reach high yields of products and thus minimize waste. Importantly, grinding minimizes environmental impact by avoiding the use of dangerous chemicals. Overall, grinding offers a scalable, cost-effective, and versatile approach to nano collagen synthesis. It facilitates precise control over particle size and high yields, making it valuable for applications in cosmetics, food supplements, regenerative medicine, and biomedical research [27–29].

The authors have recently studied the effect of extraction conditions on the characteristics of equine tendon-derived collagen which presents more advantageous qualities than collagen from other animal sources such as minimal risks of zoonosis transmission, high sequence similarity to human collagen, and higher resistance compared to other types of collagen [30]. The results of the previous work provided the starting collagen used for this study which has been focused on the post-processing of extracted partially hydrolyzed collagen and in particular on the size reduction to the nano-scale.

Partially hydrolyzed collagen derived from equine tendons offers numerous advantages over intact collagen in healthcare-related applications. Its smaller peptides enhance cellular interactions, facilitating cellular uptake and tissue integration, crucial for regenerative medicine applications. Moreover, its high biocompatibility ensures minimal risk of adverse reactions, while its biodegradability allows for gradual replacement by native tissues. Additionally, hydrolyzed collagen's ease of functionalization with bioactive molecules enables targeted delivery

Table 1
Samples description obtained from ball mill process.

Sample code	Description
0 min	Initial partially hydrolyzed powder
6 min	Powder obtained after 12 cycles of milling
12 min	Powder obtained after 24 cycles of milling
18 min	Powder obtained after 36 cycles of milling

and controlled release in drug delivery systems or wound dressings. These qualities collectively make hydrolyzed collagen a versatile and effective biomaterial for various applications, supporting advancements in biomedical research and therapeutic interventions [12,22].

The present work aims to optimize a low-cost, relatively straightforward, and environmentally conscious technique for producing nano-sized partially hydrolyzed type I collagen sourced from equine tendons and to study the effect of the mechanical treatment on its microstructure, molecular weight, size distribution, and thermal stability. Since collagen processing strongly affects its architecture at various length scales, particular attention has been paid to avoid altering the original collagen structure. As schematically reported in Fig. 1, the freeze-dried partially hydrolyzed collagen powder has been subjected to several ball mill cycles and then characterized by several techniques. To the best of the authors' knowledge, it is the first time that the effects of ball milling on the final properties of a partially hydrolyzed equine tendon-derived type I collagen have been studied.

2. Materials and methods

2.1. Production of nano collagen particles

The collagen used for this study was an experimental partially hydrolyzed type I collagen derived from equine tendons, processed through a patented spray-drying method by Typeone Biomaterials S.r.l. (Calimera, Italy). Used chemicals including sodium dodecyl sulfate (SDS), glycerol, acrylamide/bisacrylamide solution (37.5:1), bromophenol blue, Coomassie brilliant blue R-250, ammonium persulfate, *N*,*N*,*N*,*N*-tetramethyl ethylene diamine (TEMED), and 2-mercaptoethanol were sourced from Merck (Darmstadt, Germany) and Bio-Rad Laboratories (Hercules, CA, USA). A Merck KGaA's Millipore Milli-U10 water purification plant was used to produce distilled water. Additional chemical reagents employed in the study, not explicitly listed here, were also of analytical grade and procured from Merck (Darmstadt, Germany).

The size reduction was obtained by wet ball milling using distilled water. Partially hydrolyzed collagen powders were mechanically processed in a S/11000B mill, model (Ceramic Instruments S.r.l, Sassuolo Modena, Italy), with a speed of 390 rpm, in a hermetically sealed zirconia (ZrO_2) jar with zirconia grinding balls in an ambient environment. The high-energy impacts with the ZrO_2 balls finely reduced the particles to nanometric size due to the friction between the powder and the rolling balls. The milling conditions were optimized taking account of the low denaturation temperature of the partially hydrolyzed collagen, which was taken as an upper limit temperature of the milling process. It is already known in the literature that the milling process develops heat due to the friction among particles and grinding media, so a proper milling procedure was optimized to avoid excessive heat development that could denature the collagen molecules. The optimized procedure was based on a succession of milling and pause cycles. Each cycle consisted of 30 s of milling and 5 min of pause, and after every 4 cycles, the jar was cooled in the freezer for 10 min. The working temperature was always monitored (15 ± 5 °C). The mill process was extended to 36 cycles (18 min) with the goal of decreasing the size to nanometer scale, and four different samples were obtained after different milling time, as shown in Table 1. Before characterization, all samples were freeze-dried using an LIO-5P freeze-drier (Cinquepascal s.r.l., Trezzano sul Naviglio, Italy) for 24 h ($P < 100$ mTorr) and stored in a desiccator until use.

2.2. Characterization of the nano collagen particles

2.2.1. Laser diffraction

To explore the impact of milling, particle size distribution was assessed every 6 min of milling. This was done using laser diffraction technique with a CILAS 1190 laser diffractometer. For each sample, three replicates were measured to derive the average particle size.

2.2.2. Differential scanning calorimetry (DSC)

Samples underwent thermal analysis using a Mettler DSC1 Differential Scanning Calorimeter (Mettler Toledo, Greifensee, Switzerland). Approximately 5 mg of freeze-dried collagen samples were equilibrated in aluminum sample pans at 10 °C for 10 min. They were then subjected to heating at a rate of 5 °C/min from 10 °C to 100 °C under a nitrogen atmosphere [31]. For each sample, a minimum of three measurements were conducted. We defined the denaturation temperature (Td) as the peak value observed in the Heat Flow versus Temperature graph, corresponding to the endothermic phenomenon. Finally, we calculated the denaturation enthalpy (ΔH) relative to the collagen mass of the sample.

2.2.3. Scanning electron microscopy analysis (SEM)

An SEM EVO® 40 (Carl Zeiss AG, Jena, Germany) was utilized to examine the morphology of the freeze-dried powders of partially hydrolyzed collagen. Approximately 1 to 2 mg of partially hydrolyzed collagen powder was applied onto a carbon adhesive disk mounted on the stub and observed under a 20 kV accelerating voltage.

2.2.4. Atomic force microscopy analysis (AFM)

AFM characterized the surface morphology of the partially hydrolyzed collagen samples through a MultiMode 8 AFM system (Bruker, Champs sur Marne, France). AFM analysis was performed with a silicon tip on a nitride lever cantilever having a spring constant of 0.4 N/m (2 nm tip radius, 115 μm length) in the Peak Force Quantitative Nanomechanical Mapping (QNM) mode with a scanasyst-air probe. The analysis was performed on 10 % (w/v) collagen dispersions milled at different milling times, which were spin-coated onto a metallic disc and air dried [30,32]. The scanning parameters were: scan sizes of 10 × 10 μm^2 and 5 × 5 μm^2, scanning rates in the 0.640–0.574 Hz range, and resolution set at 512 lines per scan. Image J and Nanoscope Analysis v.1.5 software were used to process AFM data and quantify roughness. The roughness Ra and Rq were determined as the root mean square of z-channel fluctuations with respect to the mean height value calculated on the entire picture area. Ra and Rq for every sample were determined as the average value of 10 distinct areas of 1 × 1 μm^2.

2.2.5. Fourier transform infrared spectroscopy (FT-IR)

FT-IR spectroscopic analysis was carried out to investigate the structural organization of starting partially hydrolyzed collagen powder and nano collagen samples. A Jasco GmbH FTIR-6300 spectrometer located in Pfungstadt, Germany, was employed for the analysis About 0.2 ml of 5 % (w/v) partially hydrolyzed collagen dispersions were cast and air-dried on germanium IR lenses [30,33]. The absorbance spectra were acquired (range: 4000–400 cm^{-1}, resolution: 4.0 cm^{-1}, number of scans: 64) and analyzed by means of OriginLab software (Origin Lab Corporation, Northampton, MA, USA).

2.2.6. Sodium dodecyl-sulfate polyacrylamide gel electrophoresis (SDS-PAGE)

Variations in partially hydrolyzed collagen molecular weight across cycles were assessed through polyacrylamide gel electrophoresis with sodium dodecyl sulfate (SDS-PAGE), employing a Mini-Protean Tetra Cell System from Bio-Rad Laboratories, Inc., based in Hercules, CA, USA. Partially hydrolyzed collagen suspensions in a 1:1 ratio with Laemmli buffer and 2 M urea were treated at 50 °C for 1 h before being

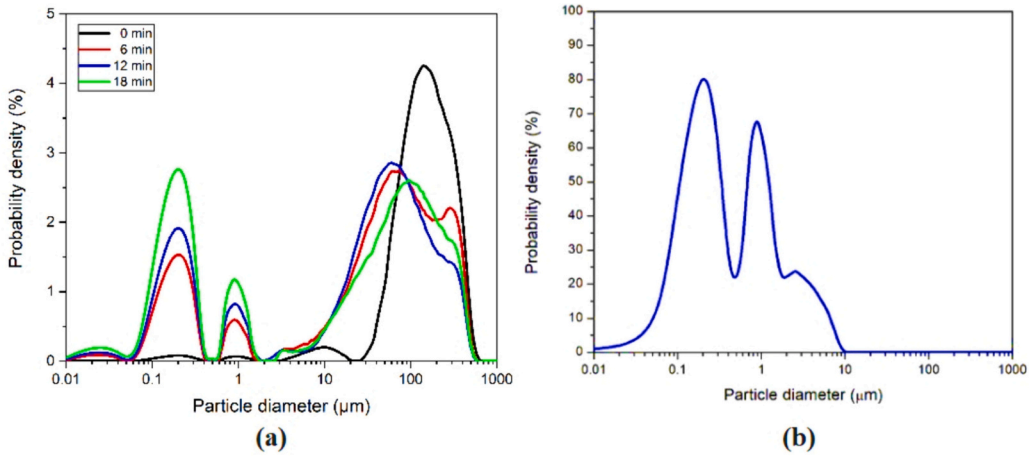

Fig. 2. a) Size distribution of partially hydrolyzed collagen particles with varying milling duration; b) size distribution after 18 min of milling and sieving.

Table 2
Particle size distribution of partially hydrolyzed collagen powders at different milling duration.

Sample code	D10 (μm)	D50 (μm)	D90 (μm)	D average (μm)
0 min	59.81 ± 3.5	156.76 ± 9.4	374.07 ± 19.5	188.26 ± 12.3
6 min	0.23 ± 0.01	58.02 ± 3.4	308.80 ± 17.6	106.48 ± 8.3
12 min	0.20 ± 0.005	43.46 ± 2.1	239.50 ± 10.2	85.38 ± 6.7
18 min	0.15 ± 0.003	37.36 ± 2.1	238.98 ± 9.4	82.89 ± 5.4
Sieved 18 min	0.050 ± 0.001	0.32 ± 0.02	2.54 ± 0.09	0.910 ± 0.001

centrifuged at maximum speed for 1 min and being loaded into the polyacrylamide gel (5 % stacking gel, 12 % resolving gel) wells [31,32]. Protein standards (10–250 kDa) were loaded to estimate the molecular weight. The polyacrylamide gel was subjected to 70 V for approximately 30 min, followed by an increase to 120 V for approximately 2.5 h before rapidly stained utilizing a previously optimized method and then acquired for further analysis [30,34,35].

2.2.7. Cell viability assessment by MTT test

Cell viability was determined by MTT test on mouse embryonic fibroblasts of the NHI/3 T3 cell line (ATCC® CRL-1658™). Cells were cultured in Dulbecco's modified Eagle medium (D-MEM) supplemented with 10 % (v/v) fetal bovine serum (FBS), 2 mM L-glutamine, and 100 μg/mL penicillin/streptomycin, in a humidified atmosphere (5 % CO_2 in air) at 37 °C. Cells (concentrated 2×10^4 per ml) were seeded in a 96-well plate and incubated with collagen or nano collagen 0.1 % in D-MEM for 24, 48, and 72 h respectively. All experiments were performed between passages 3 and 10 of propagation. At each time point, the MTT (3-(4,5-dimethylthiazol-2-yl)-2,5-diphenyltetrazolium bromide) test was performed to assess cell viability by measuring cellular metabolic activity [36]. The test evaluated the mitochondrial NAD(*P*)H-dependent oxidoreductase enzyme activity that reduced a yellow tetrazolium salt (MTT) to formazan that accumulated as crystals within healthy cells. The crystals were in turn dissolved with DMSO and the absorbance of the resulting colored solution was spectrophotometrically analyzed at 570 nm (Cytation 5, BioTek Instruments, Winooski, VT, United States). The relative viability of the cells was calculated as follows:

$$\%\textit{Relative viability of cells} = \frac{\textit{Treated cells OD}}{\textit{Control cells OD}} \times 100 \quad (1)$$

2.2.8. Statistical analysis

The experimental data were all reported as mean values together with the standard deviation. T-student test was used to analyze the statistical significance of the mean values. The differences were considered significant when $p < 0.05$.

3. Results and discussion

3.1. Size distribution analysis

The size distribution of the starting collagen powder and the milled dispersion up to 18 min of milling is reported in Fig. 2a. The density distribution illustrated the likelihood of encountering a particle with a specific diameter (D) within the given population. The original micron-sized collagen exhibited a mostly unimodal distribution centered around 200 μm. The nano-scale collagen presented a multimodal distribution pattern containing three peaks. As the milling time increased, there was a noticeable reduction in the prominence of the third peak associated with micron-sized particles. In contrast, there was a concurrent increase in the fraction of submicron and nano-scale particles. This phenomenon implied that the repeated cycles contributed to a transformation in the particle size distribution, with a diminishing presence of larger particles and a concurrent increase in the formation of smaller particles, specifically in the submicron and nano-size range. The heightened number of cycles favored the generation of finer particles, through a process that involved fragmentation or refinement of the particle sizes during the cycling procedure [12,16]. Fig. 2 presents a trimodal size distribution with a large-sized fraction that arose probably from unmilled material. Due to the peculiar nature of collagen, the optimization of the milling procedure lied in a compromise between the number of cycles and the nanometric size to preserve the original structure of the collagen. Usually, in industrial practice, ball milling involves long-lasting processes that cannot be applied to collagen otherwise the stress and temperature increase associated with milling would cause collagen denaturation. On the other hand, the procedure optimized in this work was fast and kept unaltered the collagen structure but led to a remaining unmilled material, that could be easily removed through sieving. Therefore, the trimodal distribution observed in Fig. 2a in milled collagen was modified by sieving. In this way, only one sieving step was enough to remove the fraction with a big size as reported in Fig. 2b, where the size distribution of sieved 18 min milled collagen achieved an average dimension of 0.91 μm, as also reported in modified Table 2. In this work, "nanoscale" can

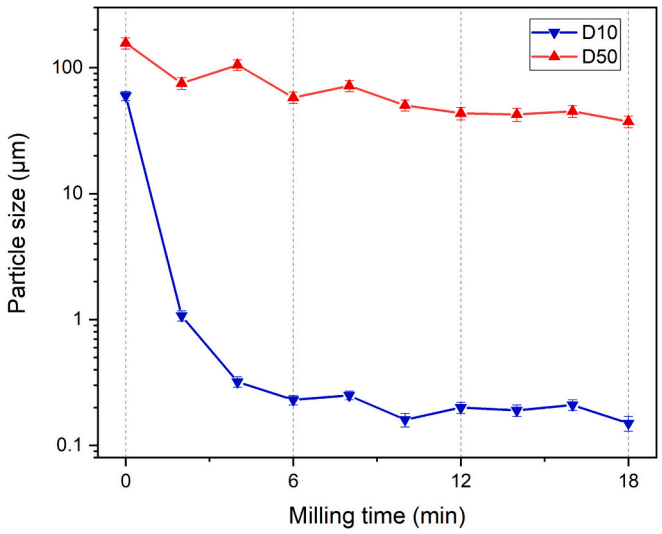

Fig. 3. Effect of milling time on D10 and D50 values of the analyzed partially hydrolyzed collagen particles.

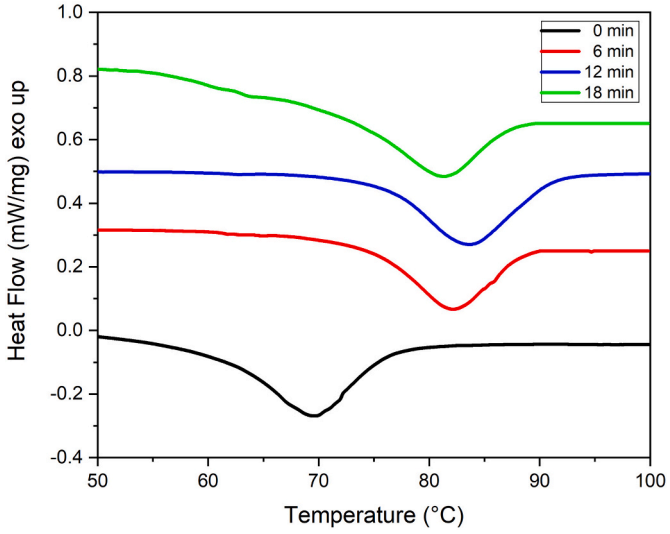

Fig. 4. DSC thermograms of collagen powders after 6, 12, and 18 min of milling.

Table 3
Thermal properties of collagen powders at different milling durations.

Sample code	T_d (°C)	ΔH (J/g)
0 min	71.8 ± 1.8	−14.4 ± 6.4
6 min	82.2 ± 2.4	−20.3 ± 4.2
12 min	83.6 ± 2.7	−26.9 ± 3.1
18 min	81.6 ± 2.2	−24.7 ± 4.3

be meant to refer to a size of less than one micron, as attested by literature on collagen nanoparticles produced by several methods, where the average size is between 200 and 400 nm [23,37,38]. It can be concluded that the proposed procedure based on ball milling can produce collagen nanoparticles.

The percentile values of the distribution, D10, D50 and D90 for the starting powder and the particles milled after 6, 12, and 18 min are reported in Table 2. These parameters can be read directly from the cumulative particle size distribution indicating the size (in microns in Table 2) below which 10 %, 50 % or 90 % of all particles are found

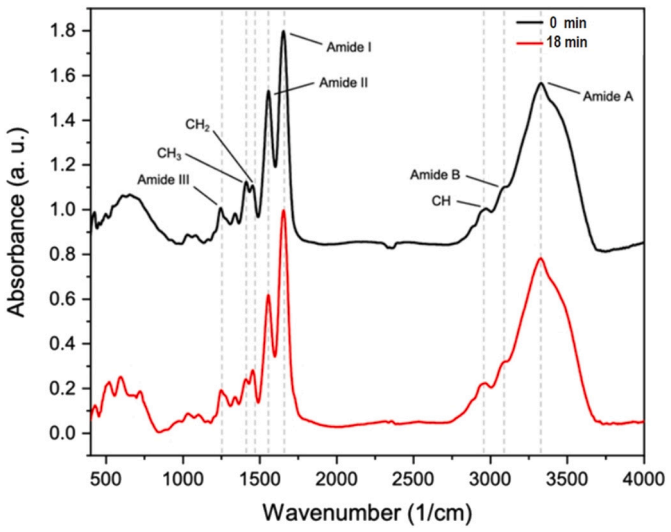

Fig. 5. FT-IR spectra of partially hydrolyzed collagen powders before and after 18 min of milling.

[39,40]. In particular, the size reduction was significant ($p < 0.05$) when comparing the percentile values of the distribution of 6 min milled collagen with the starting powder. With increasing milling time, the differences in the D10, D50 and D90 values between 12 min and 18 min were not significant ($p > 0.05$). The impact of milling cycles on the average size at different volume percentages (10 %, 50 %, and 90 %) of the particles, as determined by laser diffraction analysis carried out each 4 milling cycles, is presented in Fig. 3. This plot represents how the number of milling cycles influenced the distribution of particle sizes across different volume percentages, offering insights into the overall particle size characteristics resulting from the milling process. Due to the impact of ZrO_2 balls colliding with collagen powder, their kinetic energy was imparted to the powder particles leading to the fragmentation of larger particles and the generation of smaller ones. Naturally, the abundance of submicron and nano-sized particles increased with the milling duration.

Achieving a desired nanoparticle size distribution involves controlling the milling process, with customization possible by adjusting parameters like speed and time. This capability is particularly beneficial for applications requiring a consistent and uniform particle size distribution. It is crucial to note the concurrent increase of the temperature of the milling aqueous dispersion of collagen particles and milling media in the milling jar during the kinetic energy transfer. This temperature elevation can potentially lead to the breakdown of collagen molecular structure [23,41]. To prevent such overheating and irreversible structural damage, a precautionary measure was implemented. The milling process was intermittently paused for 5 min after every 30 s of milling, and after every 4 cycles, the jar was cooled in the freezer for 10 min. This strategic interruption and cooling regimen was adopted to preserve the collagen structure by mitigating the adverse effects of elevated temperatures during the milling process.

3.2. Calorimetric analysis

Differential Scanning Calorimetry is an effective technique for discovering the thermal stability of collagen. This test was performed on freeze-dried samples to omit the effect of water content in the milling solution. Fig. 4 shows the thermal transition of the collagen powder after 6, 12, and 18 min of milling. The temperature of the endothermic peak was associated with the denaturation temperature T_d which was found in the range of 80–84 °C for collagen samples after milling. However, it was observed at about 71 °C for the starting powder. Table 3 provides the values of T_d and enthalpy of the denaturation ΔH.

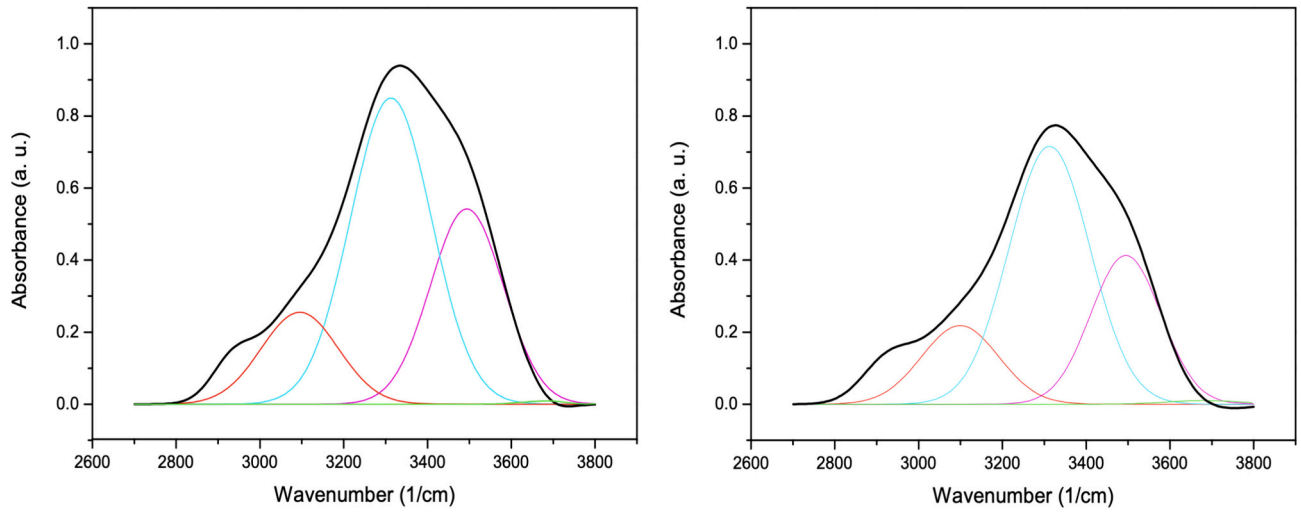

Fig. 6. Amide A peak deconvolution of samples before (left) and after 18 min of milling (right) in four components corresponding to the hydrogen bond distance of 0.31 nm (green line, at about 3700 cm^{-1}), 0.29 nm (pink line, at about 3500 cm^{-1}), 0.28 nm (light blue line, at about 3300 cm^{-1}), and 0.25 nm (red line, at about 3100 cm^{-1}).

Table 4
O—H bond distribution in partially hydrolyzed collagen before and after 36 milling cycles in the Amide A spectral range.

O—H bond length (nm)	Peak position (nm) [relative intensity area (%)]	
	0 min of milling	18 min of milling
0.31	3691 [0.5 %]	3680 [0.6 %]
0.29	3493 [29.7 %]	3494 [26.2 %]
0.28	3312 [51.6 %]	3312 [52.3 %]
0.25	3095 [14.7 %]	3099 [15.2 %]

According to the literature, freeze-dried collagen consisted of a layered structure [42]. Indeed, in these samples, large sheets of collagen were in contact with each other. It seems that the layered structure of collagen had an increasing effect on the thermal stability of the sample compared to not freeze-dried collagen. After milling, the size of partially hydrolyzed collagen particles decreased resulting in a larger contact surface area among nanoparticles compared to microparticles of the starting powder. As a consequence, this increase in the contact surface area among protein nano-aggregates leads to a rise in T_d from about 70 °C to 80 °C [43] because of new bonding formation by dehydration during freeze-drying. Reducing the particle size helped to improve the thermal stability of the partially hydrolyzed collagen since the denaturation temperature increased. This improvement is very important because partially hydrolyzed collagen often faces challenges related to thermal stability in various applications. However, a non-significant increase in both T_d and ΔH was found according to the milling cycles, suggesting that milling for 6 min was enough to reach the maximum increase of T_d obtainable with this manufacturing technique.

3.3. Structural analysis

The FT-IR spectra of collagen powders before milling and after 18 min of milling were reported in Fig. 5. As expected, the typical peaks attributable to type I collagen (Amide I: 1621–1635 cm^{-1}, C═O hydrogen-bond stretching; Amide II: 1535–1548 cm^{-1}, C—N stretching and N—H in-plane bending; Amide III: 1220–1240 cm^{-1}, N—H bending) were detected [30,33,34,44,45]. In particular, the amide I was found at 1660 cm^{-1} for 0 min and 1656 cm^{-1} for 18 min, the amide II was revealed at 1553 cm^{-1} for 0 min and 1548 cm^{-1} for 18 min, and the amide III was detected at 1242 cm^{-1} for 0 min and 1235 cm^{-1} for 18 min. Additionally, amide A and amide B were respectively found at

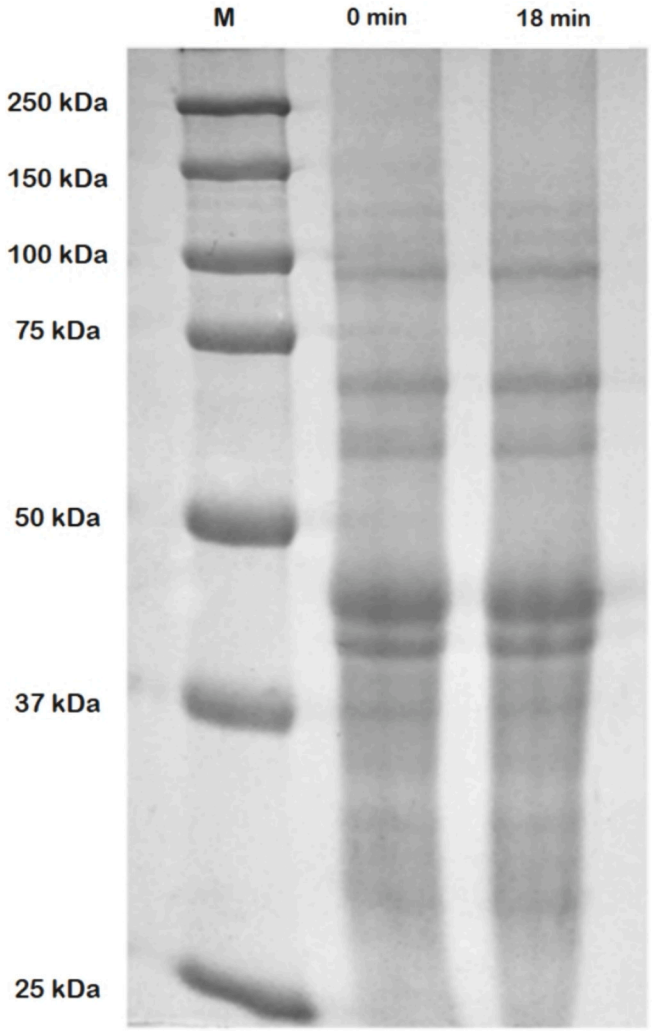

Fig. 7. Electrophoretic pattern of the partially hydrolyzed collagen powder before and after 18 min of milling compared to protein markers (M).

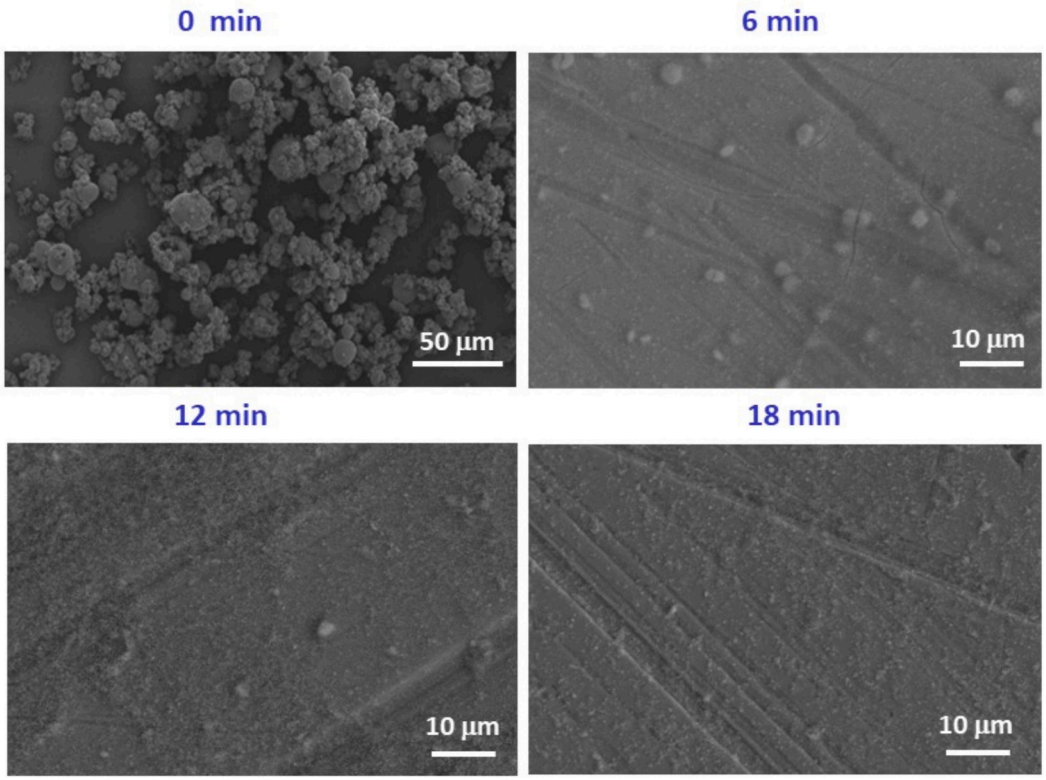

Fig. 8. Representative SEM image of the morphology of the starting and milled collagen samples.

3331 cm^{-1} and 3090 cm^{-1} for 0 min, and at 3324 cm^{-1} and 3091 cm^{-1} for 18 min [46]. The contribution at about 1080 cm^{-1}, attributable to the tensile vibrations of C═O bonds, was found in both at about 1079 cm^{-1} for 0 min and 1090 cm^{-1} for 18 min [47]. The detection of type I collagen chemical groups confirmed the nature of the material [48].

The collagen used in this study was a partially hydrolyzed type I collagen. In order to quantitatively assess the triple helical content, the amide III to -CH_2 ratio was calculated [30,46]. A ratio lower than 1 indicated the loss of the triple helical structure [49]. The starting powder was found to have a value of about 0.74, confirming the low degree of preserved triple helices. Additionally, the presence of the small peak at about 1080 cm^{-1} confirmed the nature of the partially hydrolyzed collagen that had lost its native fibrillar structure [47]. Indeed, its intensity was very low compared to the not hydrolyzed, raw, fibrillar collagen [32].

The analysis of FTIR spectra enabled also to investigate the effect of the nano collagen production protocol on the material structural conformation and its intermolecular interactions. In particular, the amide III/-CH_2 ratio of the collagen powder analyzed after 18 min of milling was found to have a value of 0.57, suggesting how a further loss of the triple helical structures content occurred [46,50]. Moreover, the increase of the C═O vibration contribution at 1080 cm^{-1} further suggested the formation of molecular aggregates or randomly organized structures [47]. Additionally, the shift of amide peaks to lower frequencies could be due to the breaking of molecular aggregates into aggregates of lower size and to the involvement of newly free -C═O and -NH groups in weaker hydrogen bonding (or long-range) interactions [51].

To deeply investigate the formation of new hydrogen bonding interactions, amides were in-depth analyzed. In particular, Amide A, which corresponded to the –OH stretching band, was deconvoluted into four components at about 3690 cm^{-1}, 3490 cm^{-1}, 3300 cm^{-1}, and 3110 cm^{-1} [33] (Fig. 6, Table 4). While the amides I, II and III were usually analyzed for the extraction of structural information, amide A, with >95 % due to the N—H stretching vibration, did not depend on the backbone conformation and thus it was very sensitive to the strength of hydrogen bonds [51]. According to the literature, the deconvoluted four frequencies ~~are~~ were related to different O—H bond lengths (3690 cm^{-1}: 0.31 nm; 3490 cm^{-1}: 0.29 nm; 3300 cm^{-1}: 0.28 nm; 3110 cm^{-1}: 0.25 nm) that corresponded to the hydrogen bonds network types around the protein [52–54]. The peaks attributable to the vapor-like state (0.31 nm) and thus to protein non-H-bonded or weakly H-bonded O—H groups were found to be very low (about 0.5 %) since collagen powders were analyzed in the dry state [52,54,55].

Otherwise, the peaks attributable to water molecules coordinated by two (0.29 nm) or three (0.28 nm) H-bonds, that formed inter- or intramolecular bridges, were found to constitute about 28 % and 52 % of the total water content respectively for both sample types. However, these contributions could be also ascribed to hydrogen bonding of –C═O groups belonging to the hydroxyl group of glycine (d(C═O—W) = 0.29 nm) and hydroxyproline (Hyp) (d(C═O—W) = 0.28 nm) residues [55]. The component at about 3110 cm^{-1} was attributed to water molecules hydrogen-bonded to polar and charged groups exposed to the macromolecule surface. This contribution was found to be about 12 % for the starting powder and about 15 % after 18 min of milling, suggesting the presence of a high number of hydrogen bonds after 18 min. Moreover, a slight increase was found in the bands intensities ratio of –CH_2 and –CH_3 (starting powder CH_2/CH_3 ratio: 0.6; cycle n.36 CH_2/CH_3 ratio: 0.9) suggesting that cross-linking reactions occurred in collagen after 18 min of milling [33,56].

3.4. Protein analysis

SDS-PAGE was conducted to analyze the protein composition of the partially hydrolyzed collagen powder and to assess the impact of the milling protocol on its molecular weight. The electrophoretic pattern of the collagen powder before milling and after 18 min of milling is depicted in Fig. 7, along with standard proteins for comparison. The

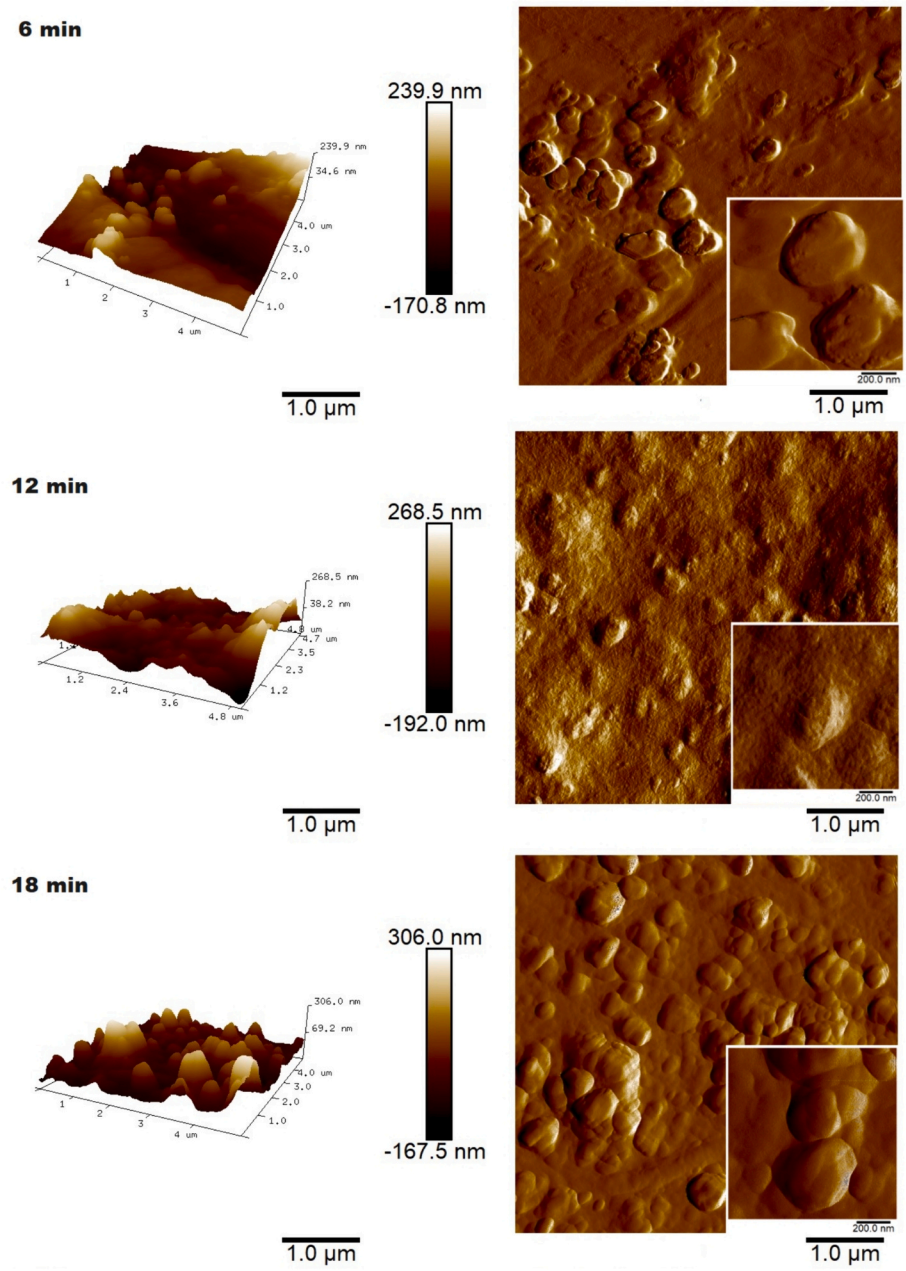

Fig. 9. AFM images of the collagen powder after different milling times at 5 × 5 μm^2 scan size. An image size of 1 × 1 μm^2 is reported in the inset.

absence of band shifts to lower molecular weights after 18 min of milling confirmed that the pointed-out protocol did not affect collagen molecular weight but only chain interaction, as emerged from the spectroscopic analysis. Although some studies were already done on the effect of ball milling on type I collagen or its hydrolysates or blends, no one of them reported an accurate investigation of their influence on its molecular weight [57–59]. Nevertheless, only a study reported the effect of milling on type II collagen molecular weight [60]. The no processing-related variations detected in the literature supported our findings.

3.5. Morphological analysis

Collagen powder morphology before and after milling was investigated both by SEM and AFM. The morphology of microparticles and the process of achieving nanoparticles involved understanding the size, shape, and structure of particles at the micrometric and nanometric levels. Milling is a mechanical process that involves reducing the size of particles through the application of mechanical forces, such as impact and attrition. When applied to microparticles to achieve nanoparticles, milling can significantly affect the morphology, size, and distribution of the particles. The primary goal of milling is to reduce the size of particles.

Microparticles were subjected to mechanical forces generated by the milling equipment, leading to fractures and breakage. As the milling process progressed, the particles underwent repeated collisions and impacts, resulting in the gradual reduction of particle size. The specific milling conditions, including the type of milling equipment, milling time, and the nature of the material being milled, ~~can~~ impacted the final particle morphology. Meanwhile, during milling, particles may have experienced agglomeration or aggregation due to attractive forces between them. It was essential to manage these phenomena to achieve a well-dispersed and stable nanoparticle suspension.

SEM analysis was carried out both on the freeze-dried starting collagen and on the milled collagen powders. As visible in Fig. 8, the

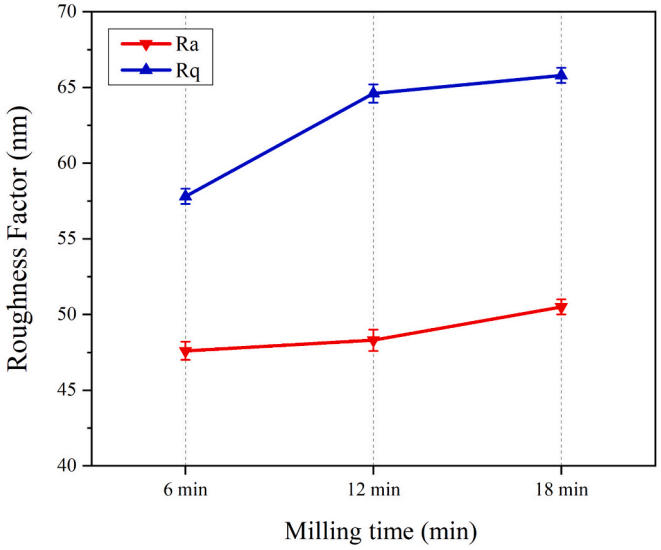

Fig. 10. Roughness factor of the collagen powder after different milling times which is obtained from NanoScope Analysis 1.5 software.

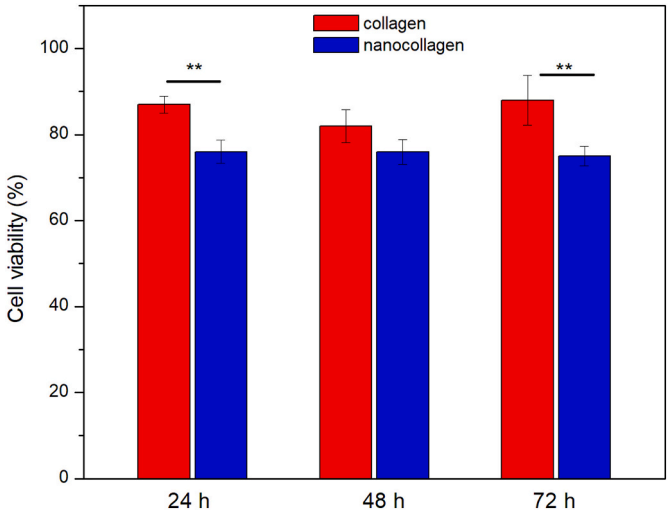

Fig. 11. Viability of 3T3 cells in the presence of partially hydrolyzed collagen and nano collagen compared to control cells (cells not exposed). (**) indicates statistical significance with $p < 0.05$.

analyzed samples consisted of almost spherical structures with different average sizes according to the processing conditions. While a significant size reduction was observed in SEM images after 6 min, no significant differences were appreciated between 12 and 18 min of milling. However, while acquiring and interpreting SEM analysis data, it should be taken into account that this morphological analysis gives a qualitative and punctual representation of the sample, which thus underestimates or overestimates the real particle size distribution. Due to this, particle size distribution data obtained from laser diffraction analysis were more accurate and reliable. Nevertheless, SEM analysis, being a morphological analysis, allowed us to spot the appearance of milled collagen powders and the effect of milling duration on them.

The AFM images of collagen after 6, 12, and 18 min of milling were reported in Fig. 9. As the number of milling cycles increased, it became evident that the size of pseudo-spherical or polyhedral collagen particles was decreasing. This observation was confirmed through the use of ImageJ analysis, and the detailed results were reported in Fig. 10. However, as the milling time increased, collagen nanoparticles, with their high contact surface, started adhering to each other.

After 18 min of ball milling, this sticking together resulted in the creation of an interwoven microstructure of collagen nanoparticles. The simultaneous reduction in size and the increased tendency of particles to stick lead to a rise in nano-scale roughness, as depicted in Fig. 10. This heightened roughness indicated an increase in surface height and elevation in the microstructure. This increase in roughness served as a rationale for improved heat transfer through contact surfaces, consequently enhancing the denaturation temperature [11].

3.6. Cell viability

The effect of milling cycles on the material biocompatibility was preliminarily assessed against 3T3 murine fibroblasts. As reported in Fig. 11, cell metabolic activity in the presence of the partially hydrolyzed collagen or nano collagen was always higher than 75–80 %, compared to control cells over the observation time, suggesting the biocompatibility of tested materials [61]. Statistically significant differences ($p < 0.05$) were found among the partially hydrolyzed collagen and nano collagen. In particular, nano collagen was found to slightly slow down fibroblast metabolic activity, probably because of its lower size and its higher ability to interact with cells. This slight reduction could be due to the material breakdown and absorption by cells [60] or to the collagen-mediated regulation of cells' catabolic and anabolic pathways. These results were consistent with those found by Klewin-Steinbock et al., who sustained the same theory and obtained comparable viability values with almost the same concentrations of horse-derived partially hydrolyzed collagen [62]. Similar results were found also by Lombardi et al. after 24 h of incubation with horse-derived partially hydrolyzed collagen [61].

4. Conclusions

In this investigation, a swift, cost-effective, straightforward, and environmentally conscious approach was employed to generate nano collagen from the equine tendon, aiming to preserve collagen integrity by controlling the temperature. Milling, a mechanical procedure involving the application of forces like impact and attrition, was utilized to decrease particle size. When applied to microparticles for nanoparticle attainment, milling significantly affected particle morphology, size, and distribution. The repetitive cycles in milling induced a refinement of the particle size distribution, reducing the prevalence of larger particles and concurrently promoting the formation of smaller particles, particularly in the submicron and nano-size range. This size reduction contributed to enhanced thermal stability in collagen, as indicated by an increase in denaturation temperature, which represented an essential improvement given collagen's thermal stability challenges in various applications. It is noteworthy that the milling process, as revealed by SDS-PAGE analysis, did not alter the partially hydrolyzed collagen's molecular weight but affected chain interactions. The simultaneous reduction in size, coupled with an increased propensity for particles to adhere, resulted in heightened nano-scale roughness. Moreover, the biocompatibility of partially hydrolyzed type I nano collagen was preliminarily assessed against 3T3 murine fibroblasts. Additional studies are still necessary to further reduce the nanometric size, optimize yields and increase the processed quantity.

CRediT authorship contribution statement

Zahra Rajabimashhadi: Writing – review & editing, Writing – original draft, Investigation, Data curation, Conceptualization. **Nunzia Gallo:** Writing – review & editing, Writing – original draft, Data curation, Conceptualization. **Francesca Russo:** Investigation, Data curation. **Sajjad Ghiyami:** Investigation, Data curation. **Claudio Mele:** Validation, Investigation, Data curation. **Maria Elena Giordano:** Investigation, Data curation. **Maria Giulia Lionetto:** Data curation, Formal

analysis, Investigation, Validation. **Luca Salvatore:** Writing – review & editing, Supervision, Methodology, Data curation. **Francesca Lionetto:** Investigation, Conceptualization, Writing – review & editing, Methodology, Data curation, Supervision.

Declaration of competing interest

This piece of the submission is being sent via mail.

Data availability

Data will be made available on request.

Acknowledgements

Typeone Biomaterials S.r.l. is kindly acknowledged for the technical support. Zahra Rajabimashhadi acknowledges Regione Puglia for funding NANOCOLLAGEN-"Development of nanometric collagen from fish industry waste" (code 284e667a) in the framework of POC PUGLIA FESR-FSE 2014/2020 RIPARTI project.

References

[1] T. Moni, Deena, J. Dayana, P. Anjana Murali, J. Jacob, D. Jose, et al., Export citation CrossMark development of antibacterial biomaterial for medical application development of antibacterial biomaterial for medical application, AIP Conf. Proc. 2263 (2020) 30012, https://doi.org/10.1063/5.0017662.
[2] A. Sionkowska, S. Skrzyński, K. Śmiechowski, A. Kołodziejczak, The review of versatile application of collagen, Polym. Adv. Technol. 28 (2017) 4–9, https://doi.org/10.1002/PAT.3842.
[3] M.A. Hussain, G. Muhammad, I. Jantan, S.N.A. Bukhari, Psyllium arabinoxylan: a versatile biomaterial for potential medicinal and pharmaceutical applications, Polym. Rev. 56 (2016) 1–30, https://doi.org/10.1080/15583724.2015.1078351.
[4] M. Milazzo, G.S. Jung, S. Danti, M.J. Buehler, Wave propagation and energy dissipation in collagen molecules, ACS Biomater. Sci. Eng. 6 (2020) 1367–1374, https://doi.org/10.1021/ACSBIOMATERIALS.9B01742.
[5] Z. Rajabimashhadi, N. Gallo, L. Salvatore, F. Lionetto, Collagen derived from fish industry waste: progresses and challenges, Polymers (Basel) 15 (2023) 544, https://doi.org/10.3390/polym15030544.
[6] T. Senadheera, D. Dave, F. Shahidi, Sea cucumber derived type I collagen: a comprehensive review, Mar. Drugs 18 (2020) 471, https://doi.org/10.3390/md18090471.
[7] B. Bhushan, Springer Handbook of Nanotechnology, 2017.
[8] H. Rohira, V. Kumar, A. Chugh, Nanotechnology: revolutionizing agricultural sector, Botanica 64 (2015) 151–155.
[9] S. Malik, K. Muhammad, Y. Waheed, Nanotechnology: a revolution in modern industry, Molecules 28 (2023) 661, https://doi.org/10.3390/MOLECULES28020661.
[10] P.R. Rauta, Y.Y.K.Y. Mohanta, D. Nayak, Nanotechnology in Biology and Medicine: Research Advancements & Future Perspectives. Illustrate, CRC Press, 2019.
[11] A. Naskar, K.S. Kim, Recent advances in nanomaterial-based wound-healing therapeutics, Pharmaceutics 12 (2020) 499, https://doi.org/10.3390/PHARMACEUTICS12060499.
[12] S. Lo, M. Fauzi, Current update of collagen nanomaterials—fabrication, characterisation and its applications: a review, Pharmaceutics 13 (2021) 1–18, https://doi.org/10.3390/pharmaceutics13030316.
[13] T. Munish, G. Ramneesh, S. Sanjeev, S. Jasdeep, S. Jaspal, G. Nikhil, Collagen based dressing and standard dressing in diabetic foot ulcer, J. Evol. Med. Dent. Sci. 4 (2015) 2278–4748, https://doi.org/10.14260/jemds/2015/521.
[14] R. Tognato, V. Bonfrate, G. Giancane, T. Serra, Fabrication of anisotropic collagen-based substrates for potential use in tissue engineering, Smart Mater. Struct. 31 (2022) 074001, https://doi.org/10.1088/1361-665X/ac701b.
[15] T.G. Sahana, P.D. Rekha, Biopolymers: applications in wound healing and skin tissue engineering, Mol. Biol. Rep. 45 (2018) 2857–2867, https://doi.org/10.1007/S11033-018-4296-3/TABLES/2.
[16] L.A. Pringgandini, G.Y. Indarti, M. Melinda, M. Sari, Effectiveness of nano-collagen spray of goldfish (Cyprinus carpio) scales waste in accelerating the incision wound healing process, J. Kedokt Gigi Univ. Padjadjaran 30 (2018) 113, https://doi.org/10.24198/jkg.v30i3.18529.
[17] Y. Ma, A. Teng, K. Zhao, K. Zhang, H. Zhao, S. Duan, et al., A top-down approach to improve collagen film's performance: the comparisons of macro, micro and nano sized fibers, Food Chem. (2020) 309, https://doi.org/10.1016/J.FOODCHEM.2019.125624.
[18] P. Katsimbri, The biology of normal bone remodelling, Eur. J. Cancer Care (Engl.) 26 (2017) e12740, https://doi.org/10.1111/ecc.12740.
[19] Wang Cheng-yue, Zhao Yuan, Yang Man, Wang Shu-feng, Nano-collagen artificial bone for alveolar ridge preservation in the Kazakh from Xinjiang Tacheng Region, Chin. J. Tissue Eng. Res. 19 (2015) 1864–1871.
[20] Shen Ling, Wang Xi-you, Yu Chen Ping, Tong., Allogeneic adipose-derived stem cells combined with nano collagen-based bone for repair of ulna bone defects, Chin. J. Tissue Eng. Res. 19 (2015) 5162–5166.
[21] M.I. Avila Rodríguez, L.G. Rodríguez Barroso, M.L. Sánchez, Collagen: a review on its sources and potential cosmetic applications, J. Cosmet. Dermatol. 17 (2018) 20–26, https://doi.org/10.1111/jocd.12450.
[22] A.B. Shekhter, A.L. Fayzullin, M.N. Vukolova, T.G. Rudenko, V.D. Osipycheva, P. F. Litvitsky, Medical applications of collagen and collagen-based materials, Curr. Med. Chem. 26 (2019) 506–516, https://doi.org/10.2174/0929867325666171205170339.
[23] W. Trilaksani, I.K.M. Adnyane, B. Riyanto, N. Safitri, Nano collagen of the grouper swim bladder in compliance with quality standard of cosmetics materials, IOP Conf. Ser. Earth Environ. Sci. 404 (2020) 012050, https://doi.org/10.1088/1755-1315/404/1/012050.
[24] S. Saallah, N.N. Naim, M.N. Mokhtar, N.F. Abu Bakar, M. Gen, W.W. Lenggoro, Transformation of cyclodextrin glucanotransferase (CGTase) from aqueous suspension to fine solid particles via electrospraying, Enzym. Microb. Technol. 64–65 (2014) 52–59, https://doi.org/10.1016/J.ENZMICTEC.2014.06.002.
[25] Haziqah Che Marzuki N, Abdul Wahab R, Abdul Hamid M. An overview of nanoemulsion: concepts of development and cosmeceutical applications. Taylor Fr Che Marzuki, RA Wahab, M Abdul HamidBiotechnology Biotechnol Equipment, 2019•Taylor Fr 2019;33:779–97. doi:https://doi.org/10.1080/13102818.2019.1620124.
[26] D. Sundaramurthi, U.M. Krishnan, S. Sethuraman, Electrospun nanofibers as scaffolds for skin tissue engineering, Polym. Rev. 54 (2014) 348–376, https://doi.org/10.1080/15583724.2014.881374.
[27] S.K. Mhetar, A. Ashok Nerle, R.L. Patil, R.A. Pawar, M.M. Patil, H.T. Shinde, Cost effective ball milling machine for producing nanopowder, Int. Res. J. Eng. Technol. 4 (2017) 330–334.
[28] M. Kumar, X. Xiong, Z. Wan, Y. Sun, D.C.W. Tsang, J. Gupta, et al., Ball milling as a mechanochemical technology for fabrication of novel biochar nanomaterials, Bioresour. Technol. 312 (2020) 123613, https://doi.org/10.1016/J.BIORTECH.2020.123613.
[29] F. Lionetto, C. Esposito Corcione, A. Rizzo, A. Maffezzoli, Production and characterization of polyethylene terephthalate nanoparticles, Polymers 13 (2021) 3745, https://doi.org/10.3390/polym13213745.
[30] L. Salvatore, F. Russo, M.L. Natali, Z. Rajabimashhadi, S. Bagheri, C. Mele, et al., On the effect of pepsin incubation on type I collagen from horse tendon: fine tuning of its physico-chemical and rheological properties, Int. J. Biol. Macromol. 256 (2024) 128489, https://doi.org/10.1016/j.ijbiomac.2023.128489.
[31] N. Gallo, M.L. Natali, A. Quarta, A. Gaballo, A. Terzi, T. Sibillano, et al., Aquaponics-derived tilapia skin collagen for biomaterials development, Polymers (Basel) 14 (2022) 1865, https://doi.org/10.3390/POLYM14091865/S1.
[32] L. Salvatore, N. Gallo, D. Aiello, P. Lunetti, A. Barca, L. Blasi, et al., An insight on type I collagen from horse tendon for the manufacture of implantable devices, Int. J. Biol. Macromol. 154 (2020) 291–306, https://doi.org/10.1016/J.IJBIOMAC.2020.03.082.
[33] C.T. Prontera, N. Gallo, R. Giannuzzi, M. Pugliese, V. Primiceri, F. Mariano, et al., Collagen membrane as water-based gel electrolyte for electrochromic devices, Gels 9 (2023) 310.
[34] N. Gallo, M.L. Natali, C. Curci, A. Picerno, A. Gallone, M. Vulpi, et al., Analysis of the physico-chemical, mechanical and biological properties of crosslinked type-i collagen from horse tendon: towards the development of ideal scaffolding material for urethral regeneration, Materials (Basel) (2021) 14, https://doi.org/10.3390/MA14247648.
[35] A.M. Lawrence, H. Besir, Staining of proteins in gels with Coomassie G-250 without organic solvent and acetic acid, JoVE (J. Vis. Exp.) (2009) e1350, https://doi.org/10.3791/1350.
[36] P.W. Sylvester, Optimization of the tetrazolium dye (MTT) colorimetric assay for cellular growth and viability, Drug Des. Discov. Methods Protoc. (2011) 157–168, https://doi.org/10.1007/978-1-61779-012-6_9.
[37] Shalaby M, Ghareeb AZ, Khedr SM, Mostafa HM, Saeed H, Hamouda D, et al. Nanoparticles of bioactive natural collagen for wound healing: experimental approach. BiorxivOrgM Shalaby, AZ Ghareeb, SM Khedr, HM Most H Saeed, D HamoudabioRxiv, 2023•biorxivOrg n.d. doi:https://doi.org/10.1101/2023.02.21.529363.
[38] Sumarto Desmelati, Dahlia Dewita, Sari P.A. Syafrijal, Determination of nano-collagen quality from sea cucumber *Holothuria scabra*, IOP Conf. Ser. Earth Environ. Sci. 430 (2020) 012005, https://doi.org/10.1088/1755-1315/430/1/012005.
[39] F. Lionetto, M.G. Lionetto, C. Mele, C.E. Corcione, S. Bagheri, G. Udayan, et al., Autofluorescence of model polyethylene terephthalate nanoplastics for cell interaction studies, Nanomaterials 12 (2022) 1560, https://doi.org/10.3390/nano12091560.
[40] F. Lionetto, C. Esposito Corcione, F. Messa, S. Perrone, A. Salomone, A. Maffezzoli, The sorption of amoxicillin on engineered polyethylene terephthalate microplastics, J. Polym. Environ. 31 (2023) 1383–1397, https://doi.org/10.1007/s10924-022-02690-0.
[41] X. Wang, Y. Yan, M.J. Yost, S.A. Fann, S. Dong, X. Li, Nanomechanical characterization of micro/nanofiber reinforced type I collagens, J. Biomed. Mater. Res. Part A 83 (2007) 130–135, https://doi.org/10.1002/jbm.a.31207.
[42] H. Van Duong, T.T.L. Chau, N.T.T. Dang, Nguyen D. Van, S.L. Le, T.S. Ho, et al., Self-aggregation of water-dispersible nanocollagen helices, Biomater. Sci. 6 (2018) 651–660, https://doi.org/10.1039/C7BM01141E.
[43] M. Vedhanayagam, M. Nidhin, N. Duraipandy, N.D. Naresh, G. Jaganathan, M. Ranganathan, et al., Role of nanoparticle size in self-assemble processes of

collagen for tissue engineering application, Int. J. Biol. Macromol. 99 (2017) 655–664, https://doi.org/10.1016/j.ijbiomac.2017.02.102.
[44] M. Carbonaro, A. Nucara, Secondary structure of food proteins by Fourier transform spectroscopy in the mid-infrared region, Amino Acids 38 (2010) 679–690, https://doi.org/10.1007/S00726-009-0274-3/FIGURES/4.
[45] Vidal B. De Campos, M.L.S. Mello, Collagen type I amide I band infrared spectroscopy, Micron 42 (2011) 283–289, https://doi.org/10.1016/J.MICRON.2010.09.010.
[46] T. Riaz, R. Zeeshan, F. Zarif, K. Ilyas, N. Muhammad, S.Z. Safi, et al., FTIR analysis of natural and synthetic collagen, Appl. Spectrosc. Rev. 53 (2018) 703–746, https://doi.org/10.1080/05704928.2018.1426595.
[47] Y.A. Nashchekina, A.A. Starostina, N.A. Trusova, M.Y. Sirotkina, A.I. Lihachev, A. V. Nashchekin, Molecular and fibrillar structure collagen analysis by FTIR spectroscopy, J. Phys. Conf. Ser. 1697 (2020) 012053, https://doi.org/10.1088/1742-6596/1697/1/012053.
[48] K. Belbachir, R. Noreen, G. Gouspillou, C. Petibois, Collagen types analysis and differentiation by FTIR spectroscopy, Anal. Bioanal. Chem. 395 (2009) 829–837, https://doi.org/10.1007/S00216-009-3019-Y.
[49] Y. Li, X. Dong, L. Yao, Y. Wang, L. Wang, Z. Jiang, et al., Preparation and characterization of nanocomposite hydrogels based on self-assembling collagen and cellulose nanocrystals, Polymers (Basel) 15 (2023) 1308, https://doi.org/10.3390/polym15051308.
[50] Z.S.S. Júnior, S.B. Botta, P.A. Ana, C.M. França, K.P.S. Fernandes, R.A. Mesquita-Ferrari, et al., Effect of papain-based gel on type I collagen - spectroscopy applied for microstructural analysis, Sci. Rep. 5 (2015) 11448, https://doi.org/10.1038/srep11448.
[51] C. Şendrea, M. Niculescu, C. Carşote, E. Badea, A. Adams, H. Iovu, Non-invasive Characterisation of Collagen-based Materials by NMR-mouse and ATR-FTIR, 2016.
[52] K. Nakamoto, M. Margoshes, R.E. Rundle, Stretching frequencies as a function of distances in hydrogen bonds, J. Am. Chem. Soc. 77 (1955) 6480–6486, https://doi.org/10.1021/ja01629a013.
[53] Bridelli M, Stani C, Biological RB-J of, 2017 undefined. Fourier transform infrared conformational investigation of type I collagen aged by in vitro induced dehydration and non-enzymatic glycation treatments. PagepressjournalsOrgMG Bridelli, C Stani, R BedottiJournal Biol Res Della Soc 2017•pagepressjournalsOrg 2017;90:45–50. doi:https://doi.org/10.4081/jbr.2017.6254.
[54] M.G. Bridelli, Fourier transform infrared spectroscopy in the study of hydrated biological macromolecules, in: Fourier Transform - High-Tech Appl Curr Trends, 2017, https://doi.org/10.5772/66576.
[55] M.G. Bridelli, P.R. Crippa, Infrared and water sorption studies of the hydration structure and mechanism in natural and synthetic melanin, J. Phys. Chem. B 114 (2010) 9381–9390, https://doi.org/10.1021/jp101833k.
[56] H. Sideroudi, G. Labiris, A. Soto-Beobide, G. Voyiatzis, A. Chrissanthopoulos, V. Kozobolis, The effect of collagen cross-linking procedure on the material of intracorneal ring segments, Curr. Eye Res. 40 (2015) 592–597, https://doi.org/10.3109/02713683.2014.941071.
[57] S.P. Dwivedi, A. Saxena, S. Sharma, G. Singh, J. Singh, M. Mia, et al., Effect of ball-milling process parameters on mechanical properties of Al/Al2O3/collagen powder composite using statistical approach, J. Mater. Res. Technol. 15 (2021) 2918–2932, https://doi.org/10.1016/j.jmrt.2021.09.082.
[58] G. Dindelegan, C. Popa, I. Brie, K. Magyari, V. Simon, Milling effects on hybrid collagen/inorganic phase composites, Mater. Sci. Forum 672 (2011) 129–132, https://doi.org/10.4028/www.scientific.net/MSF.672.129.
[59] B. Liu, Y. Li, Q. Wang, S. Bai, Green fabrication of leather solid waste/thermoplastic polyurethanes composite: physically de-bundling effect of solid-state shear milling on collagen bundles, Compos. Sci. Technol. 181 (2019) 107674, https://doi.org/10.1016/j.compscitech.2019.06.001.
[60] Y. Wang, S. Yang, L. Zhang, F. Yuan, L. Mao, J. Liu, et al., Effects of different mechanical processes on the structural and powdery properties of insoluble undenatured type II collagen, Food Chem. 406 (2023) 135068, https://doi.org/10.1016/j.foodchem.2022.135068.
[61] F. Lombardi, P. Palumbo, F.R. Augello, I. Giusti, V. Dolo, L. Guerrini, et al., Type I collagen suspension induces neocollagenesis and myodifferentiation in fibroblasts *in vitro*, Biomed. Res. Int. 2020 (2020) 1–11, https://doi.org/10.1155/2020/6093974.
[62] S. Klewin-Steinböck, A. Nowak-Terpiłowska, Z. Adamski, K. Grocholewicz, M. Wyganowska-Świątkowska, Effect of injectable equine collagen type I on metabolic activity and apoptosis of gingival fibroblasts, Adv. Dermatol. Allergol. 38 (2021) 440–445, https://doi.org/10.5114/ada.2020.94256.